Bound states of charmed baryons and antibaryons*

C. B. Dover, S. H. Kahana, and T. L. Trueman
Brookhaven National Laboratory, Upton, New York 11973
(Received 17 March 1977)

Within the framework of nonrelativistic potential models, we investigate the possibility that bound states of the type $\bar{B}_c B_c$ may exist, where B_c is a charmed member of the $\underline{20}$ baryon multiplet of SU(4). By rather general considerations, we establish the approximate level order of the bound-state spectrum. Specific potential models are then invoked to qualitatively estimate the binding energies and rms radii of $\bar{B}_c B_c$ bound states. For reasonably small binding energies ($\leq 1/2$ GeV), for which a potential description is sensible, such configurations are found to be "quasimolecular" in nature, i.e., having rms radii considerably larger (≥ 0.7 fm) than the corresponding $\bar{c}c$ quark-model states. We show that most of the low-lying states are isospin $I = 0$ as in the $\bar{c}c$ model. However, because of the coherent effect of tensor forces, certain $I = 1$ configurations of the $\bar{C}_1 C_1$ system experience a downward energy shift, and hence could appear in the same energy region as $I = 0$ states (e.g., $^{2I+1,2S+1}L_J = {}^{33}P_0$ state near $^{13}P_{0,1,2}$ states). The states we describe can mix with and modify the properties of $\bar{c}c$ quark states of the same quantum numbers in the $J/\psi,\chi,\psi'$ region from 3.1 to 3.7 GeV. Some of them could appear independently as narrow states in the mass region of 4 GeV. "Exotic" $\bar{C}_1 C_1$ states with $I = 2$ are shown to always lie above $I = 0,1$ configurations of the same L; however, for a wide class of potential models, the P-wave $\bar{C}_1 C_1$ states ($^{53}P_{0,1,2}$,$^{51}P_1$) are still bound close to threshold (~ 4.8 GeV). We exhibit qualitative arguments that some of these $\bar{B}_c B_c$ bound states may be narrow. We discuss possible experimental means for finding the $I = 1$ and 2 states, i.e., those *not* predicted by the $c\bar{c}$ quark model.

I. INTRODUCTION AND MOTIVATION

The experimental discovery of the J/ψ, χ, and ψ' mesons[1] pointed to the existence of the charm quantum number, and led to model calculations of these states[2] as bound states of a charmed-quark-antiquark ($\bar{c}c$) pair (the "charmonium" picture). The subsequent discoveries of charmed baryons[3] and charmed mesons[4] lend credence to these calculations and to the idea of an approximate underlying SU(4) symmetry. The existence of these charmed baryons B_c and mesons M_c invites one to consider the possibility of additional mesons formed as bound states of $\bar{B}_c B_c$ or $\bar{M}_c M_c$ systems. These states could share the quantum numbers of a $\bar{c}c$ system, but would be quite different in structure: We envisage here relatively loosely bound $\bar{B}_c B_c$ systems of a "quasimolecular" character, whose spatial extent is generally large compared to that of $\bar{c}c$ systems. Such a possibility was considered by Feinberg and Lee,[5] who studied states of the type $\bar{F}F$, bound by a sum of two phenomenologically adjusted square-well potentials. Here F is a new heavy fermion, not necessarily contained in an SU(4) structure. More recently, states of the type $\bar{D}D$ have been considered by several authors,[6] where D is a particular charmed meson. In the present article, we consider the possibility of bound and/or resonant states $\bar{B}_c B_c$ of a charmed baryon B_c and its antiparticle. Here B_c is specifically a charmed member of the $\underline{20}$ baryon multiplet of SU(4).

The framework for our discussion is nonrelativistic potential theory. We argue that potential theory should be a good approximation for weakly bound $\bar{B}_c B_c$ systems because of the large mass m_{B_c} of the charmed baryons. As we show explicitly later, the potential $V(r)$ operating in a $\bar{B}_c B_c$ system is close to the static limit of spin-independent central forces. The central forces alone are already sufficient to support the existence of a considerable number of S-, P-, and D-wave bound states. The tensor (S_{12}) and spin-orbit ($L \cdot S$) forces, of order $(\mu/2m_{B_c})^2 \approx 0.01$–$0.03$ for $\mu \approx 750$ MeV, in most cases produce only rather small energy splittings of states of different spin S and total angular momentum J.

Several authors[7] have considered similar treatments of the nucleon-antinucleon ($N\bar{N}$) system based on potentials obtained from the NN problem via the G-parity transformation. The NN potential is taken as the sum of pseudoscalar-, scalar-, and vector-meson exchanges, with coupling constants adjusted to give a best fit to NN scattering data and the properties of the deuteron. We envisage a parallel treatment of $\bar{B}_c B_c$ systems. However, it is important to remark at the outset that such an approach is only well justified for low-energy, near-mass-shell processes. Thus our emphasis is on systems whose binding energy is small compared to their rest mass $2m_B$. Our hope is that such systems *close to threshold* will remain as relatively pure $\bar{B}B$ states when we allow mixing with other configurations. "Bootstrap"

calculations have been attempted, using a set of relativistic Blankenbecler-Sugar equations,[8] in which the low-lying mesons themselves ($\pi, \rho, \omega, \ldots$) appear as *deeply* bound states corresponding to some appropriate superposition of $\bar{N}N$, $\bar{\Lambda}\Lambda$, $\bar{\Sigma}\Sigma$, etc. configurations. Our approach is more modest and not in conflict with the underlying quark structure of the baryons; we restrict our attention to the possibility of $\bar{B}_c B_c$ quasimolecular states close to the threshold, where a potential description should be valid. For the $\bar{N}N$ system, there are several likely candidates for both bound and resonant quasimolecular states near threshold.[9] Several of these have been interpreted in terms of eigenstates of nonrelativistic potential models.[10]

To extend the $\bar{N}N$ calculations[7,10] to $\bar{B}_c B_c$ systems we employ an SU(4) framework. An intermediate step, using SU(3) to estimate binding energies for $\bar{N}N$, $\bar{\Lambda}\Lambda$, $\bar{\Sigma}\Sigma$, and $\bar{\Xi}\Xi$ systems, has already received some attention.[11] Our justification for ultimately considering the charmed baryons in isolation is their large mass. The large mass differences between the N, Λ, Σ, and Ξ masses and the charmed-baryon masses implies a large SU(4) breaking. One result of this is that $\bar{B}_c B_c$ threshold states lie very high in mass compared to other $\bar{B}B$ configurations, and would be expected to mix only with other $\bar{B}_c B_c$ states. In our calculations, SU(4) symmetry is invoked only as a means of relating unknown charmed-baryon–meson coupling constants to couplings phenomenologically determined from uncharmed-baryon-baryon scattering data (mostly NN, some $\Delta N, \Sigma N$). One may of course question *any* retention of SU(4) symmetry; however, we intend to show that certain features of the level spectrum are independent of detailed assumptions about coupling constants. It is these general features of the potential and its spectrum which we wish to emphasize.

The $\bar{B}_c B_c$ states considered here and the $c\bar{c}$ states of the quark model are of course not distinct in general. Our calculations suggest that these classes of states may interweave somewhat in energy. Hence, if $\bar{B}_c B_c$ and $c\bar{c}$ systems possess the same quantum numbers, they will mix. Such mixing is probably largest for S states, in which case $\bar{B}_c B_c$ states may not possess a separate existence. The quasimolecular picture we propose is more sensible for P, D, etc. states, for which the centrifugal barrier acts to keep the baryon and antibaryon well separated, and to retard somewhat the mixing with the corresponding $c\bar{c}$ state.

This paper is organized as follows: In Sec. II, we define the general form of potential model which we consider for the configurations

$$\bar{B}_c B_c = \{\bar{C}_0 C_0,\ \bar{C}_1 C_1,\ \bar{S}S,\ \bar{A}A,\ \bar{T}T,\ \bar{X}X,\ \bar{X}_s X_s\}\ ;$$

the notation is defined in the Appendix. We isolate the dominant terms corresponding to the static limit. This enables us to establish that in general isospin $I=0$ states lie lowest, followed by $I=1$ states, and at still higher energies, $I=2$ states ($\bar{C}_1 C_1$ only). The presence of tensor (S_{12}) and spin-orbit ($\vec{L}\cdot\vec{S}$) forces induces energy splittings among states of given I. We show that for all $I=0$ states, the tensor forces due to various meson exchanges act coherently, so that in a given channel they are either all repulsive or all attractive. The dominance of S_{12} over $\vec{L}\cdot\vec{S}$ forces for $\bar{B}_c B_c$ systems in $I=0$ states enables us to establish the level order for spin $S=1$ states, independent of detailed assumptions about coupling constants. For $I=1$ states, there is no coherence of S_{12} or $\vec{L}\cdot\vec{S}$ forces, except for $\bar{C}_1 C_1$, and hence energy splittings are smaller. We show that the $\bar{C}_1 C_1$ system is of special interest, since both $I=0$ and $I=1$ states exhibit coherence of tensor forces. One $I=1$ level for each L is pushed down by this coherent effect (e.g., $^{33}P_0$) and mingles with $I=0$ states. Estimates indicate that "exotic" $I=2$ states of the $\bar{C}_1 C_1$ system may also be bound, although much less than $I=0$, 1 states. The possibility of $I=1$ or $I=2$ bound states is a distinctive feature of the $\bar{B}_c B_c$ model; these states cannot be produced in the $c\bar{c}$ model.

In Sec. III, we present the results of some representative potential-model calculations. Absolute binding energies are found to be very sensitive to details of the short-range cutoff of the potential. This emphasizes that such models are unreliable for deeply bound states, e.g. those involving small separations of $\bar{B}_c$ and B_c. However, level order is preserved for a wide range of cutoff prescriptions. Most of the low-lying $\bar{B}_c B_c$ states are predicted to lie in the energy region from 4 to 5 GeV, although the possibility exists that $\bar{B}_c B_c$ states may mix with $c\bar{c}$ states in the J/ψ region from 3 to 4 GeV.

II. POTENTIAL MODELS FOR $\bar{B}_c B_c$–GENERAL FEATURES

In this section, we briefly sketch the procedure used to generate a potential for any $\bar{B}B$ system. We represent the overall potential, except for annihilation processes, as a sum of one-boson-exchange potentials, represented schematically in Fig. 1. We include the exchange of all nonstrange mesons with masses ≤ 1 GeV; these are the pseudoscalar, scalar, and vector mesons indicated in Fig. 1. These exchanges are responsible for the longer-range part of the BB and $\bar{B}B$ potentials. We omit the effects of coupled channels and obtain a local, energy-independent approximation to the potential by starting with the relat-

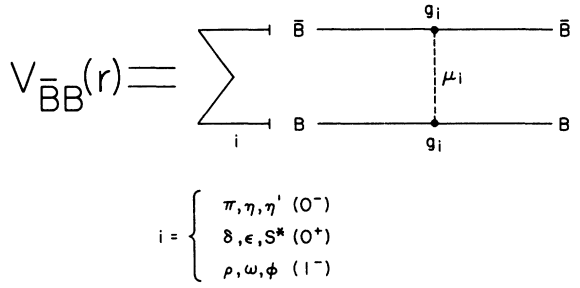

FIG. 1. A schematic representation of the one-boson-exchange (OBE) model for the antibaryon-baryon $\bar{B}B$) potential $V_{\bar{B}B}(r)$. We include the exchange of the pseudoscalar, scalar, and vector mesons indicated in the figure. These exchanges are iterated to all orders by solving the nonrelativistic Schrödinger equation with the potential $V_{\bar{B}B}(r)$ as input.

ivistic Hamiltonians H_P, H_S, H_V and performing a nonrelativistic reduction in the usual way.[12] Here H_P couples baryons to the pseudoscalar mesons (π,η,η') and is given by

$$H_P = ig\bar{\psi}\gamma_5\psi\phi, \tag{2.1}$$

where $\bar{\psi}$ and ψ are Dirac spinors for the baryons, ϕ is the meson field, and g is a dimensionless coupling constant. For the scalar mesons (δ,ϵ,S^*) we have

$$H_S = g\bar{\psi}\psi\phi, \tag{2.2}$$

and for baryon couplings to vector mesons (ρ,ω,φ) we have

$$H_V = ig\bar{\psi}\gamma_\mu\psi\phi^\mu + \frac{f}{4M}\bar{\psi}\sigma_{\mu\nu}\psi(\partial^\mu\phi^\nu - \partial^\nu\phi^\mu). \tag{2.3}$$

In Eq. (2.3), γ_μ is the usual Dirac matrix, $\sigma_{\mu\nu} = [\gamma_\mu,\gamma_\nu]/2i$, f and g are dimensionless coupling constants, and M is a scale mass.

In the nonrelativistic limit, we obtain the following contributions[12] to the real part of the $\bar{B}B$ potential to order $(\mu_i/2m_B)^2$, where μ_i = meson mass and m_B = baryon mass: For pseudoscalar exchange between spin-$\frac{1}{2}$ fermions, we have

$$V^i_{\bar{B}B}(r) = P_i(\vec{\sigma}_1\cdot\vec{\sigma}_2 V^i_0(r) + S_{12}V^i_{S_{12}}(r)), \tag{2.4}$$

where $\vec{\sigma}_1\circ\vec{\sigma}_2 = -3$ or $+1$ for spin $S=0$ or 1, respectively, and $S_{12} = 3(\vec{\sigma}_1\circ\hat{r})(\vec{\sigma}_2\cdot\hat{r}) - (\vec{\sigma}_1\circ\vec{\sigma}_2)$ is the tensor-force operator. Further, we have

$$\begin{aligned} &V^i_0(r) = \mu_i(g_i^2/4\pi)\beta_i^2\phi(x_i)/3, \\ &V^i_{S_{12}}(r) = \mu_i(g_i^2/4\pi)\beta_i^2\chi(x_i), \\ &\phi(x_i) = e^{-x_i}/x_i, \\ &\chi(x_i) = \left(\frac{1}{3}+\frac{1}{x_i}+\frac{1}{x_i^2}\right)\phi(x_i), \end{aligned} \tag{2.5}$$

where $x_i = \mu_i r$ and $\beta_i = \mu_i/2m_B$. For scalar-meson exchange, we have

$$V^i_{\bar{B}B}(r) = -P_i[V^i_0(r) + \vec{L}\cdot\vec{S}V^i_{LS}(r)], \tag{2.6}$$

where

$$\begin{aligned} &V^i_0 = \mu_i(g_i^2/4\pi)\phi(x_i), \\ &V^i_{LS}(r) = \mu_i(g_i^2/4\pi)\beta_i^2\xi(x_i), \\ &\xi(x_i) = 2\left(\frac{1}{x_i}+\frac{1}{x_i^2}\right)\phi(x_i), \end{aligned} \tag{2.7}$$

and $\vec{L}\cdot\vec{S} = -(L+1)$, -1, L for $S=1$ and $J=L-1$, L, $L+1$, respectively. Finally, for vector-meson exchange, we obtain

$$\begin{aligned} V^i_{\bar{B}B}(r) = -P_i[&V^i_0(r) + \vec{\sigma}_1\cdot\vec{\sigma}_2 V^i_o(r) \\ &- S_{12}V^i_{S_{12}}(r) - \vec{L}\cdot\vec{S}V^i_{LS}(r)], \end{aligned} \tag{2.8}$$

where

$$\begin{aligned} &V^i_0(r) = \mu_i[(g_i+\beta_i^2 f_i)^2/4\pi]\phi(x_i), \\ &V^i_o(r) = \mu_i[(g_i+f_i)^2/4\pi]2\beta_i^2\phi(x_i)/3, \\ &V^i_{S_{12}}(r) = \mu_i[(g_i+f_i)^2/4\pi]\beta_i^2\chi(x_i), \\ &V^i_{LS}(r) = \mu_i[(g_i^2+4g_if_i/3+\beta_i^2f_i^2)/4\pi]3\beta_i^2\xi(x_i). \end{aligned} \tag{2.9}$$

Equation (2.9) follows if we assume that the scale mass M in Eq. (2.3) is replaced by m_B. If we instead assume that M is the same for each $\bar{B}B$ system (chosen equal to proton mass in Ref. 12), then we must replace $f_i\beta_i$ by $f_i\beta_i m_B/M$ in Eq. (2.9). In Eqs. (2.4), (2.6), and (2.8), the isospin factor P_i is defined by

$$P_i = \begin{cases} 1 \ (\eta,\eta',\omega,\varphi,\epsilon,S^*), \\ -\vec{T}_1\cdot\vec{T}_2 \ (\pi,\rho,\delta), \end{cases} \tag{2.10}$$

where $\vec{T}_1\cdot\vec{T}_2 = -3$ or $+1$ for total isospin $I=0$ or 1 states, respectively, of two isospin-$\frac{1}{2}$ particles. For isospin-1 particles ($\bar{\Sigma}\Sigma$ or $\bar{C}_1C_1$), we have $\vec{T}_1\cdot\vec{T}_2 = -2$, -1, or $+1$ for $I=0$, 1, or 2, respectively. In this paper, we only consider systems composed of a baryon B and its own antibaryon $\bar{B}$. One could also consider more general configurations $\bar{B}_iB_j$, where $i\neq j$; such configurations could produce bound states with the quantum numbers of strange or charmed mesons. In particular the coupled $\bar{C}_1C_1$ and $\bar{C}_1C_0$ systems for $I=1$ should be considered together; this would lead to some additional levels.

Because of the G-parity invariance of the strong interactions, the diagonal potentials $V^i_{\bar{B}B}(r)$ are related to the corresponding baryon-baryon potentials $V^i_{BB}(r)$ by

$$V^i_{\bar{B}B}(r) = (-1)^{G_i}V^i_{BB}(r), \tag{2.11}$$

where G_i is the G parity of the ith meson ($G=-1$ for $\pi,\omega,\varphi,\delta$; $G=+1$ for $\eta,\eta',\rho,\epsilon,S^*$). Note that the systems we consider do not involve kaon ex-

change. Equation (2.11) relates the nonannihilation part of the $\bar{B}B$ potential to the corresponding BB potential. We are thus able to take advantage of the extensive phenomenological analyses of baryon-baryon scattering (particularly NN, and to a lesser extent, ΛN and ΣN) to obtain values for the various coupling constants g_i. For instance numerous analyses[13] of NN scattering have been performed within the context of the one-boson-exchange potential (OBEP). A more extended analysis of NN, ΛN, and ΣN data has been carried out by de Swart and collaborators,[12] using SU(3) to relate various coupling constants. From the analysis of Ref. 12 and Eq. (2.11), one is able to construct potentials for $\bar{N}N$, $\bar{\Lambda}\Lambda$, $\bar{\Sigma}\Sigma$, and $\bar{\Xi}\Xi$ systems.[11] The extension to $\bar{B}_cB_c$ systems with charmed baryons involves additional assumptions. In the Appendix, we show how SU(4) invariance applied to coupling constants enables us to relate the unknown constants $g_{i\bar{B}_cB_c}$ to known coupling strengths g_{iNN} of mesons to nucleons. In addition to the real potentials $V^i_{\bar{B}B}(r)$ generated by meson exchange, the $\bar{B}B$ potential contains an annihilation piece which has no analog for BB systems. The annihilation processes into multimeson intermediate states determine the hadronic width of the $\bar{B}_cB_c$ configurations we consider, and to some extent shift the binding energies. We treat this question qualitatively in Sec. IV.

Let us consider some of the qualitative features of the meson-exchange potentials, with an eye toward establishing some general properties which are independent of detailed assumptions about the coupling constants g_i. First compare $\bar{B}_cB_c$ to $\bar{N}N$ in the same state. If the potential $V(r)$ were the same for the two systems, the $\bar{B}_cB_c$ configuration would be more deeply bound, since the kinetic energy term in the Schrödinger equation ($\sim 1/m_B$) is smaller for $\bar{B}_cB_c$ than for $\bar{N}N$. Calculations on the $\bar{N}N$ system based on realistic NN potentials suggest a rich spectrum of bound states for several models.[7] One should also then expect a variety of $\bar{B}_cB_c$ bound states.

For the $\bar{N}N$ system, the recoil corrections to the static limit ($\vec{\sigma}_1\circ\vec{\sigma}_2$, $\vec{L}\circ\vec{S}$, and S_{12} forces) are not negligible, since $(\mu_i/2m_N)^2\approx\frac{1}{7}$ for a typical mass $\mu_i = 750$ MeV ($\approx\rho,\omega,\epsilon$ exchange). For $\bar{B}_cB_c$ systems, on the other hand, we are much closer to the static limit, since $(\mu_i/2m_{B_c})^2\approx 0.01$ to 0.03 for $m_{B_c}\approx 2$–4 GeV. Thus the terms V_0^i in Eqs. (2.7) and (2.9) provide the most important parts of the $\bar{B}_cB_c$ potential. The weaker spin-orbit and tensor forces produce splittings of levels of different J and S, but in most cases are not able to produce binding by themselves. For any $\bar{B}_cB_c$ system, the dominant static limit assumes the form [see Eqs. (2.6) and (2.8)]

$$V_{\bar{B}_cB_c}(r) = -V_0^{\omega}(r) - V_0^{\varphi}(r) - V_0^{\epsilon}(r) - V_0^{S*}(r) + \vec{T}_1\cdot\vec{T}_2[V_0^{\rho}(r) + V_0^{\delta}(r)]. \tag{2.12}$$

Two important points are evident from Eq. (2.12):

(1) In the static limit, *all* isoscalar-meson exchanges generate *attraction* for *any* $\bar{B}B$ system. As we show explicitly later, this part of the potential is already sufficient to produce bound states. Note that this *coherence* of isoscalar exchanges is absent in the BB system, since the terms $V_0^{\omega}(r)$ and $V_0^{\varphi}(r)$ become *repulsive*, so in general there is much less attraction than for the corresponding $\bar{B}B$ system.

(2) For $\vec{T}_1\circ\vec{T}_2<0$, the isovector-exchange terms (ρ,δ) are also attractive. For isospin-$\frac{1}{2}$ fermions, this means that $I=0$ states correspond to maximum attraction (*all* isoscalar and isovector terms are individually attractive). For $I=1$ states, isovector-meson exchange is repulsive, tending to cancel out some of the attraction from isoscalar exchange. For isospin-1 fermions, i.e., Σ and C_1, $\vec{T}_1\cdot\vec{T}_2<0$ for *both* $I=0,1$. Thus some $I=1$ states of $\bar{\Sigma}\Sigma$ and $\bar{C}_1C_1$ are also expected to be bound because of the coherent attractive effect of all terms $V_0^i(r)$.

In the static limit, where $V(r)$ depends on isospin I but not S or J, the following picture thus emerges: In general, independent of the choice of coupling constants, $I=0$ states of any $\bar{B}B$ system will lie lower in energy than $I=1$ states. For $\bar{\Sigma}\Sigma$ and $\bar{C}_1C_1$ systems, $I=2$ states occur at still higher energies, since the coherent central attraction characteristic of $I=0$ and some $I=1$ states is absent. The partial cancellation which always occurs between isoscalar- and isovector-meson exchange terms provides a mechanism for shifting the exotic $I=2$ states to higher energies (they can still be weakly bound, however, as shown in Sec. III). Using Eq. (2.12), we obtain for $\bar{C}_1C_1$ or $\bar{\Sigma}\Sigma$ systems the result

$$V^{I=2}_{\bar{C}_1C_1}(r) - V^{I=0}_{\bar{C}_1C_1}(r) = 3[V^{I=1}_{\bar{C}_1C_1}(r) - V^{I=0}_{\bar{C}_1C_1}(r)]. \tag{2.13}$$

Now let $u(r)$ be the radial wave function for a $\bar{C}_1C_1$ bound state generated by isoscalar exchange only. The splitting between $I=0$ and 1 states induced by isovector exchange is then

$$\Delta = \int_0^{\infty} u^2(r)[V_0^{\rho}(r) + V_0^{\delta}(r)] \tag{2.14}$$

in perturbation theory. From Eq. (2.13), we would then predict that $I=2$ states of $\bar{C}_1C_1$ would lie at an energy 3Δ above that for $I=0$ states.

It should also be noted that Eq. (2.13) also holds if we include $\vec{\sigma}_1\circ\vec{\sigma}_2$, $\vec{L}\circ\vec{S}$, and S_{12} forces, as long as we compare potentials corresponding to the

same L, S, and J. Thus, for instance, Eq. (2.13) enables us to predict that the $^{53}P_0$-$^{13}P_0$ splitting for $\overline{\Sigma}\Sigma$ or $\overline{C}_1C_1$ is three times that for $^{33}P_0$-$^{13}P_0$. Here we use the notation $^{2I+1,2S+1}L_J$ to denote a $\overline{B}_cB_c$ configuration. These predictions are a good check on the numerical results presented in Sec. III.

An estimate of Δ can be obtained by assuming that $u(r)$ is sharply localized at some radius R. We then obtain roughly

$$\Delta \approx V_0^{\rho}(R) + V_0^{\delta}(R). \tag{2.15}$$

Using the coupling constants for the two models discussed in Sec. III, and $R \approx 0.7$ fm, we obtain values of Δ in the range 100–200 MeV. This is a crude estimate of the isospin splitting between $I=0$ and $I=1$ states of the $\overline{C}_1C_1$ system induced by central forces alone.

In addition to the isospin splittings coming from the central forces, energy splittings of states of the same I and L but different S and J are induced by the tensor (S_{12}) and spin-orbit ($\vec{L}\cdot\vec{S}$) forces. An inspection of Eqs. (2.4)–(2.9) reveals the following *coherence property* of the tensor forces for *any* $\overline{B}B$ system:

For $\vec{T}_1\cdot\vec{T}_2 < 0$ and $S=1$, the diagonal tensor forces arising from *each* meson exchange are of the *same* sign. For $S_{12}<0$ ($J=L\pm1$), all tensor forces are *attractive*, while for $S_{12}>0$ ($J=L$), they are all repulsive.

For $L=1$, for example, $S_{12}=-4,+2,-\frac{2}{5}$ for $J=L-1$, $L, L+1$, respectively. Hence the coherent attraction in $J=L-1$ states from tensor forces is 10 times stronger than for $J=L+1$ states, For $\vec{T}_1\cdot\vec{T}_2>0$, on the other hand, there is a tendency for tensor forces to cancel (π,η of opposite sign, ρ,ω of opposite sign). Also, for $\overline{B}B$ systems, there is no coherence property of $\vec{L}\cdot\vec{S}$ or $\vec{\sigma}_1\cdot\vec{\sigma}_2$ forces for any I, i.e., there are always as many attractive as repulsive contributions. Another type of coherence is also evident from Eqs. (2.4)–(2.9) for states with $S=1$, $\vec{T}_1\cdot\vec{T}_2<0$:

Within a given nonet, *all* components of the force (central, $\vec{L}\cdot\vec{S}, S_{12}$) are of one sign in certain states. We find all vector-meson exchanges (ρ,ω,φ) attractive for $J=L-1$, all pseudoscalar exchanges (π,η,η') repulsive for $J=L$, and all scalar exchanges (δ,ϵ,S^*) attractive for $J=L+1$.

These coherence properties enable us to predict which states of a $\overline{B}_cB_c$ system must lie lowest in energy, independent of the choice of coupling constants and masses. The general features of $\overline{B}_cB_c$ spectra which hold for *any* potential model of the one-boson-exchange type are the following:

(1) $I=0$ states (with certain exceptions detailed below) lie lower in energy than $I=1$ or $I=2$ states.

(2) The state with $I=0, S=1, J=L-1$ always lies lowest for any $\overline{B}_cB_c$ system of a given L. The configurations of maximum diagonal attraction are thus $^{2I+1,2S+1}L_J = {}^{13}P_0$, $^{13}D_1$, $^{13}F_2$, $^{13}G_3$, etc. The off diagonal tensor coupling of $^{13}D_1$ to $^{13}S_1$, $^{13}F_2$ to $^{13}P_2$, etc., provides additional attraction.

(3) The coherence of tensor forces implies a level structure $J=L-1$ (lowest), $J=L+1$, $J=L$ (highest) for $I=0$, $S=1$ states. For $L=1$, this means an ordering $^{13}P_0$, $^{13}P_2$, $^{13}P_1$. The ordering $^{13}P_0$, $^{13}P_1$, $^{13}P_2$ characteristic of a strong spin-orbit force is not normally attained for $\overline{B}_cB_c$ systems because of the absence of any overall coherence in $\vec{L}\cdot\vec{S}$ forces. However, for $\vec{T}_1\cdot\vec{T}_2<0$, the vector-meson $\vec{L}\cdot\vec{S}$ forces are coherent and attractive, while the scalar-meson $\vec{L}\cdot\vec{S}$ forces are also coherent but of the opposite sign. The ordering $^{13}P_0$, $^{13}P_1$, $^{13}P_2$ can be produced if vector $\vec{L}\cdot\vec{S}$ forces are sufficiently dominant over scalar ones. This is the case for some one-boson-exchange models.[13]

Let us now look at tensor and spin-orbit splittings. Consider the states $|LSJ\rangle$ and $|LSJ'\rangle$ of *any* $\overline{B}B$ system. If we compare states of the same isospin ($\vec{T}_1\cdot\vec{T}_2$), the energy difference due to S_{12} forces in perturbation theory is

$$\{\langle LSJ'|S_{12}|LSJ'\rangle - \langle LSJ|S_{12}|LSJ\rangle\}\Delta_{S_{12}},$$

where

$$\Delta_{S_{12}} = \int_0^{\infty} u^2(r)[-\vec{T}_1\cdot\vec{T}_2 V^{\pi}_{S_{12}}(r) - \vec{T}_1\cdot\vec{T}_2 V^{\rho}_{S_{12}}(r) + V^{\eta}_{S_{12}}(r) + V^{\eta'}_{S_{12}}(r) + V^{\omega}_{S_{12}}(r) + V^{\varphi}_{S_{12}}(r)]dr. \tag{2.16}$$

In Eq. (2.6), $u(r)$ is the radial wave function generated by the central potential alone, as in Eq. (2.14). Note the coherent effect in Eq. (2.16) for $\vec{T}_1\cdot\vec{T}_2<0$, according to the above discussion. The spin-orbit splitting between the same two states is $\{\langle LSJ'|\vec{L}\cdot\vec{S}|LSJ'\rangle - \langle LSJ|\vec{L}\cdot\vec{S}|LSJ\rangle\}\Delta_{LS}$, where

$$\Delta_{LS} = \int_0^{\infty} u^2(r)[-\vec{T}_1\cdot\vec{T}_2 V^{\rho}_{LS}(r) + V^{\omega}_{LS}(r) + V^{\varphi}_{LS}(r) + \vec{T}_1\cdot\vec{T}_2 V^{\delta}_{LS}(r) - V^{\epsilon}_{LS}(r) - V^{S*}_{LS}(r)]\,. \tag{2.17}$$

Note the tendency of the $\vec{L}\cdot\vec{S}$ forces to cancel (no overall coherence) for any value of $\vec{T}_1\cdot\vec{T}_2$. Thus we expect, in most cases, that the largest splitting of $I=0$ states is due to tensor forces. However,

Δ_{LS} is quite model-dependent, since it involves cancellations among sizable contributions. For most models,[13] the dominant contribution to Δ_{LS} is from (ρ,ω) exchange. For strong vector cou-

plings, Δ_{LS} can be comparable to $\Delta_{S_{12}}$ even in the absence of coherence. If $\vec{T}_1 \cdot \vec{T}_2 > 0$, there are no coherent effects and hence tensor and spin-orbit splittings are comparable and rather small.

States with $S=0$ are of course not shifted by $\vec{L}\cdot\vec{S}$ or S_{12} forces. Hence they should lie close to the unperturbed position of the $S=1$ configurations. In particular, since the $S=1$, $J=L$, $L+1$ configurations are shifted in opposite directions by S_{12} and $\vec{L}\cdot\vec{S}$ forces, we expect the $^{11}P_1$, $^{13}P_1$, and $^{13}P_2$ states to appear at comparable energies. As we see later, only the $^{13}P_0$ state is shifted downward by both $\vec{L}\cdot\vec{S}$ and S_{12} forces.

For $\bar{C}_1 C_1$ or $\bar{\Sigma}\Sigma$ systems ($I=1$ baryons), coherence of tensor forces occurs for *both* $I=0$ *and* $I=1$, although the $I=0$ state still lies lowest. As is clear from Eqs. (2.16) and (2.17), only the configuration of *minimum* J is shifted downward by both S_{12} and (vector-dominated) $\vec{L}\cdot\vec{S}$ forces. For $J=L$ and $J=L+1$, S_{12} and $\vec{L}\cdot\vec{S}$ forces produce shifts of opposite sign. Thus for $I=1$, $S=1$, the $J=L-1$ state must always lie lowest. Thus for $\bar{C}_1 C_1$, or $\bar{\Sigma}\Sigma$, the $^{33}P_0$, $^{33}D_1$, etc., states are the lowest-lying $I=1$ states for each L. Basing our estimates on Eqs. (2.16) and (2.17), we find that S_{12} and $\vec{L}\cdot\vec{S}$ splittings are comparable to the isospin splittings produced by central forces alone [see Eqs. (2.14) and (2.15)]. One would expect the $^{33}L_{L-1}$ configurations of $\bar{C}_1 C_1$ or $\bar{\Sigma}\Sigma$ to lie at energies comparable to or lower than $^{13}L_L$ or $^{13}L_{L+1}$ states. The lowest-lying states of the $\bar{B}B$ model are thus not necessarily all $I=0$ states, as in the charmonium picture. Our considerations provide a *unique* set of quantum numbers ($^{33}P_0$) for the lightest of such heavy $I=1$ mesons (with $L\neq 0$). The prediction of such relatively low-lying states not encompassed by the $\bar{c}c$ model is perhaps the most interesting feature of the $\bar{B}B$ model.

III. MODEL CALCULATIONS OF THE SPECTRUM OF $\bar{B}_c B_c$ BOUND STATES

In this section, we present the results of some preliminary model calculations of the $\bar{B}_c B_c$ bound-state spectrum. We remark at the outset that the *absolute binding energies* which one obtains are quite sensitive to detailed assumptions concerning the choice of coupling constants and the short-range cutoff (or regularization) used for the potential. However, the *level orderings* of the lowest-lying states and their *quantum numbers* are less model-dependent, and are predictable from the general arguments of Sec. II.

We restrict our attention here to bound states of the type $\bar{B}_c B_c$, where B_c is *charmed* baryon belonging to the $\underline{20}$ representation of SU(4) and $\bar{B}_c$ is the antiparticle of B_c. In the notation of the Appendix, B_c includes the $I=0$ members C_0, T, and X_s, the $I=\frac{1}{2}$ members A, S, and X, and the $I=1$ member C_1. Again, we note that systems of the type $\bar{B}_i B_{i'}$, where B_i and $B_{i'}$ are distinct baryons, are omitted. Such systems would also be interesting to study, since bound states with the quantum numbers of strange or charmed mesons could be formed. One would also expect additional "nondiagonal" bound states such as $C_1\,\bar{C}_0$, which have no net strangeness or charm, but which correspond to quantum numbers not attainable in the charmonium model (here $I=1$).

For the specific systems we consider, the diagonal potential $\bar{B}_c B_c \to \bar{B}_c B_c$ is mediated only by the exchange of the usual nonstrange and noncharmed mesons ($\pi, \eta, \eta', \rho, \omega, \varphi, \delta, \epsilon, S^*$, etc.). Strange- and charmed-meson exchange contribute only to channel couplings (e.g., $\bar{C}_1 C_1 \to \bar{S}S$ via K exchange), which we ignore. We also do not include channel couplings induced by the exchange of the usual mesons (e.g., $\bar{C}_1 C_1 \to \bar{C}_0 C_0$ via π exchange). Such couplings could have a sizable effect on absolute binding energies. However, since the uncertainties due to the choice of coupling constants and short-range behavior are large, it seems unnecessary to include channel couplings in this first stage of investigation.

In this article, we consider two specific models for generating the potentials $V(r)$ for various $\bar{B}_c B_c$ configurations. In the modified Bryan-Phillips (BP) model,[14] we start from the phenomenological static nucleon-nucleon (NN) potential of Bryan and Scott[15] and perform the G-parity transformation of Eq. (2.11) to construct the corresponding $\bar{N}N$ potential.[7] This potential is then of the one-boson-exchange form of Eqs. (2.4) to (2.10) for $r > r_0$, where r_0 is a cutoff radius. For $r < r_0$ in the BP model, the potential $V(r)$ is set equal to zero. We now note that any other diagonal $\bar{B}B \to \bar{B}B$ potential in such a model will be of the same radial form and involve exchanges of the same mesons, except that the recoil corrections $\sim(\mu/2M)^2$ are evaluated with a mass $M=m_B$ rather than $M=m_N$ and different coupling constatns are used. We now require that the coupling constants satisfy the particular form of SU(4) symmetry discussed in the Appendix. The coupling of each meson in the $\underline{15}$ representation of SU(4) to the baryons in the $\underline{20}$ representation is described by three parameters $g/\sqrt{4\pi}$, α, and θ as in SU(3). In addition, the coupling $g_1/\sqrt{4\pi}$ to the meson in $\underline{1}$ is required. In the BP model, we are given only the couplings of the pseudoscalar (P), vector (V), and scalar (S) nonets to the nucleon. We now pick the $[F/(D+F)]$ ratio α and the mixing angle θ for each nonet in order to be consistent with SU(4). This requires

$$
\begin{aligned}
3-4\alpha_P &= \sqrt{3}(\cos\theta_P g_{NN\eta} + \sin\theta_P g_{NN\eta'})/g_{NN\pi}\,,\\
3-4\alpha_V^e &= \sqrt{3}(\cos\theta_V g_{NN\varphi} + \sin\theta_V g_{NN\omega})/g_{NN\rho}\,,\\
3-4\alpha_V^m &= \sqrt{3}(\cos\theta_V f_{NN\varphi} + \sin\theta_V f_{NN\omega})/f_{NN\rho}\,,\\
3-4\alpha_S &= \sqrt{3}(\cos\theta_S g_{NNS^*} + \sin\theta_S g_{NN\epsilon})/g_{NN\delta}\,.
\end{aligned}
\tag{3.1}
$$

For the BP model, we have the nucleon coupling constants $g_{NN\pi}/\sqrt{4\pi}=3.42$, $g_{NN\eta}/\sqrt{4\pi}=2.646$, $g_{NN\rho}/\sqrt{4\pi}=0.825$, $g_{NN\omega}/\sqrt{4\pi}=4.637$, $f_{NN\rho}/\sqrt{4\pi}=3.628$, $g_{NN\delta}/\sqrt{4\pi}=2.47$, $g_{NN\epsilon}/\sqrt{4\pi}=3.066$; other couplings are taken to be zero. If we use the usual pseudoscalar mixing angle $\theta_P=-10.4°$,[12,16] Eq. (3.1) gives $\alpha_P=0.421$. For vector couplings, we use the ideal mixing angle $\theta_V=\tan^{-1}(1/\sqrt{2})$; Eq. (3.1) then yields $\alpha_V^e=-0.656$ and $\alpha_V^m=\frac{3}{4}$. For scalar couplings,[12,17] we use $\theta_S=0$ and hence $\alpha_S=\frac{3}{4}$. The scale mass M in Eq. (2.3) is taken to be M_{B_c} for each $\bar{B}_cB_c$ configuration.

The other OBEP model we consider is due to Nagels, Rijken, and de Swart[12]; we refer to it as the NRD model. These authors have performed a simultaneous fit to NN, ΛN, and ΣN scattering, using the physical masses for N, Λ, and Σ, but constraining the coupling constants by SU(3). The potentials are of the form of Eqs. (2.4)–(2.9), with an additional quadratic spin-orbit potential of order $(\mu/2M)^4$; this term is very small for the systems considered here. For $r\le r_c$, the BB potential is taken to be infinitely repulsive, i.e., a hard core of radius r_c. For $\bar{B}B$ systems, this model does not provide us with a prescription for constructing $V(r)$ for $r\le r_c$. In this paper, we retain the condition that the wave function vanish at $r=r_c$ for $\bar{B}_cB_c$ systems. This assumption is rather arbitrary. For S states, the results are particularly sensitive to the choice of cutoff and are hence only schematic. It is clear that a properly regularized potential should be used. The values of α, θ and the meson couplings to the nucleon are taken from Ref. 12. They are $g_{NN\pi}/\sqrt{4\pi}=3.66$, $g_{NN\eta}/\sqrt{4\pi}=2.73$, $g_{NN\eta'}/\sqrt{4\pi}=3.89$, $\theta_P=-10.4°$, $\alpha_P=0.515$, $g_{NN\rho}/\sqrt{4\pi}=0.594$, $g_{NN\omega}/\sqrt{4\pi}=3.37$, $g_{NN\varphi}/\sqrt{4\pi}=-1.12$, $f_{NN\rho}/\sqrt{4\pi}=4.82$, $f_{NN\omega}/\sqrt{4\pi}=2.34$, $f_{NN\varphi}/\sqrt{4\pi}=-0.51$, $\theta_V=\tan^{-1}(1/\sqrt{2})$, $\alpha_V^e=0$, $\alpha_V^m=\frac{2}{3}$, $g_{NN\epsilon}/\sqrt{4\pi}=5.03$, $\theta_S=0$; other scalar couplings are zero. In this model,[12] the effects of the large widths of the ρ and ϵ are taken into account; the scale mass M in Eq. (2.3) is taken to be the proton mass for all $\bar{B}_cB_c$ configurations.

The coupling constants of the four lightest charmed baryons (C_0, C_1, A, S) are displayed in Tables I and II for the extended versions of the Bryan-Phillips (BP) and Nagels-Rijken-de Swart (NRD) models, respectively. The most striking difference between the two models lies in the coupling to scalar mesons. In the NRD model, the ϵ is universally coupled to all the baryons, and the δ and S^* couplings are zero. In the BP model, on the other hand, the ϵ couplings are smaller than for the NRD model, but the δ and S^* have nonzero couplings.

TABLE I. Coupling constants of mesons to C_0, C_1, A, S in extended Bryan-Phillips model ($g_\pi = g_{BB\pi}/\sqrt{4\pi}$, etc.).

	C_0	C_1	A	S
g_π	0	3.96	1.02	1.98
g_η	0.86	2.26	−0.86	−1.12
$g_{\eta'}$	−1.72	−0.38	−1.40	0.24
g_ρ	0	2.73	1.73	1.37
f_ρ	0	1.81	−0.91	0.91
g_ω	3.45	2.73	1.73	1.37
f_ω	−1.81	1.81	−0.91	0.91
g_φ	0	0	−2.44	−1.93
f_φ	0	0	1.28	−1.28
g_δ	0	1.23	−0.62	0.62
g_ϵ	2.06	4.07	2.06	4.07
g_{S^*}	−0.71	0.71	0.36	−0.36

We take the following masses for the charmed baryons: $m_{C_0}=2.26$ GeV,[3] $m_{C_1}=2.42$ GeV,[3] $m_A=2.47$ GeV, $m_S=2.57$ GeV, $m_T=2.73$ GeV.[18] The lowest $\bar{B}_cB_c$ thresholds that we consider are at 4.52 GeV ($\bar{C}_0C_0$) and 4.84 GeV ($\bar{C}_1C_1$). Note that the $\bar{C}_1C_0$ threshold at 4.68 GeV would lead to additional $I=1$ bound states in this region. Quasimolecular $\bar{B}_cB_c$ mesons are *a priori* expected to occur in the mass region above 4 GeV; structures between 3 and 4 GeV would be strongly bound and thus would mix with the corresponding $\bar{c}c$ states of the charmonium model. We also note from Tables I and II that only C_1 and S couple strongly to the pion. Although the dominant mechanism for binding is the coherent central attraction from ω and ϵ exchange and the pion exchange potential by itself is not usually sufficient to bind a $\bar{B}_cB_c$ state with $L\ge 1$, it does serve to increase the *number* of bound states. The long range of the pion term also en-

TABLE II. Coupling constants of mesons to C_0, C_1, A, S in extended model of Nagels, Rijken, and de Swart.

	C_0	C_1	A	S
g_π	0	3.55	0.52	1.78
g_η	1.01	2.81	0.13	−0.22
$g_{\eta'}$	2.19	3.95	2.35	4.50
g_ρ	0	1.19	0.59	0.59
f_ρ	0	3.21	−0.54	1.61
g_ω	2.78	2.78	2.18	2.18
f_ω	−0.35	3.93	0.19	2.33
g_φ	−1.12	−1.12	−1.96	−1.96
f_φ	−0.51	−0.51	0.25	−2.78
g_ϵ	5.03	5.03	5.03	5.03

ables the $\bar{B}_c B_c$ wave function to be localized at larger distances, and hence is largely responsible for the sizable rms radius of these states. Thus we expect the $\bar{C}_1 C_1$ and $\bar{S}S$ systems to support the greatest number of bound states with the largest amount of binding.

We now discuss the general features of the numerical results. We first note that there is no reason to take the cutoff parameters r_0 and r_c of the BP and NRD models to be equal for the corresponding $\bar{B}B$ and BB systems. For $\bar{B}B$, we have more attraction at short distances than for BB. For the BP potential, for instance, we would expect that the appropriate value of r_0 [$V(r)=0$ for $r \leq r_0$] would be *smaller* for $\bar{B}B$ than for BB, to account for this increased attraction. We have in general calculated binding energies as a function of r_0 or r_c; here we present results for choices of these parameters.

As noted in Sec. II, the dominant ω- and ϵ-exchange central forces are always *coherent* and *attractive* for *any* $\bar{B}B$ system. In the NRD model, the ϵ coupling is universal (same for all B) and very strong. In Fig. 2, we show the spectrum of $\bar{B}_c B_c$ $L=1$ and 2 bound states in the BP model produced by including *only* the *central* forces generated by *isoscalar*-meson exchange. The spin-dependent part of the central force $(\sim \vec{\sigma}_1 \cdot \vec{\sigma}_2)$ typically produces only (30–40)-MeV splittings, so all (S,J,T) combinations for a given L are essentially degenerate in this approximation. The main point of Fig. 2 is that the *coherence* of spin- and isospin-independent Wigner forces $(\omega,\varphi,\epsilon)$ is already sufficient to produce binding of $L=1$ or 2 states of almost all $\bar{B}_c B_c$ configurations (and also some states of higher L). The large mass of the charmed baryons makes it easier to produce binding with a given potential, and also leads to a smaller splitting between $L=1$ and $L=2$ states, compared to the corresponding $\bar{N}N$ states,[7] for instance. Thus in such nonrelativistic potential models, we expect bound states near *any* $\bar{B}_c B_c$ threshold.

The size of the energy splitting $\Delta\epsilon_{\text{cent}}$ of P and D states in Fig. 2 can be simply understood in terms of the difference in centrifugal potentials $L(L+1)/m_B r^2$, evaluated at the localization radius $r=R$ of the wave function. We find

$$\Delta\epsilon_{\text{cent}} \approx 4/m_B R^2 . \tag{3.2}$$

Inserting $m_B \approx 2.26$ GeV and $R \approx 0.7$ fm, we find $\Delta\epsilon_{\text{cent}} \approx 140$ MeV for $\bar{C}_0 C_0$, in good accord with the exact results in Fig. 2. Since $\Delta\epsilon \sim 1/m_B$, the centrifugal splittings become very small for weakly bound (large R) systems with large rest mass (large m_B).

In Fig. 2, we give only the energies of *bound* states. Because of the large mass of the charmed baryons, and the consequent reduction of the centrifugal barrier (relative to $\bar{N}N$, for instance), the elastic width for $\bar{B}_c B_c$ resonant states becomes

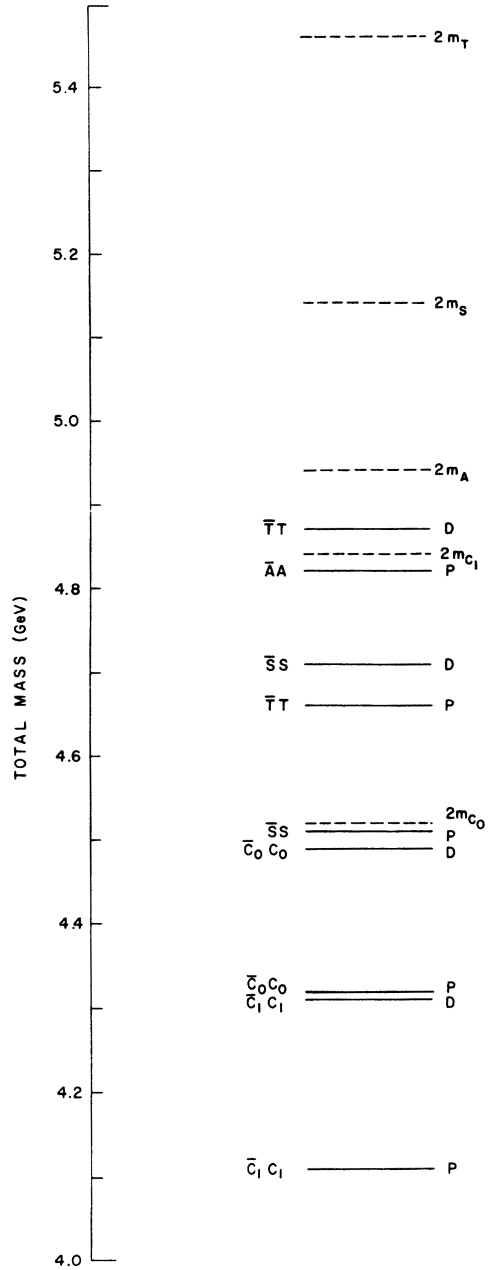

FIG. 2. Spectrum of $\bar{B}_c B_c$ bound states for $L=1$ (P) and $L=2$ (D) with isoscalar central forces only. We used the Bryan-Phillips potential with a cutoff $r_0=0.456$ fm. The $\vec{\sigma}_1 \cdot \vec{\sigma}_2$ component of the central potential produces splittings of only 30–40 MeV, so states of different spin S and isospin I but the same L are essentially degenerate. The $L=2$ states of $\bar{A}A$ are unbound. The various thresholds are shown as dashed lines. We have omitted the bound states of $\bar{X}X$ and $\bar{X}_s X_s$.

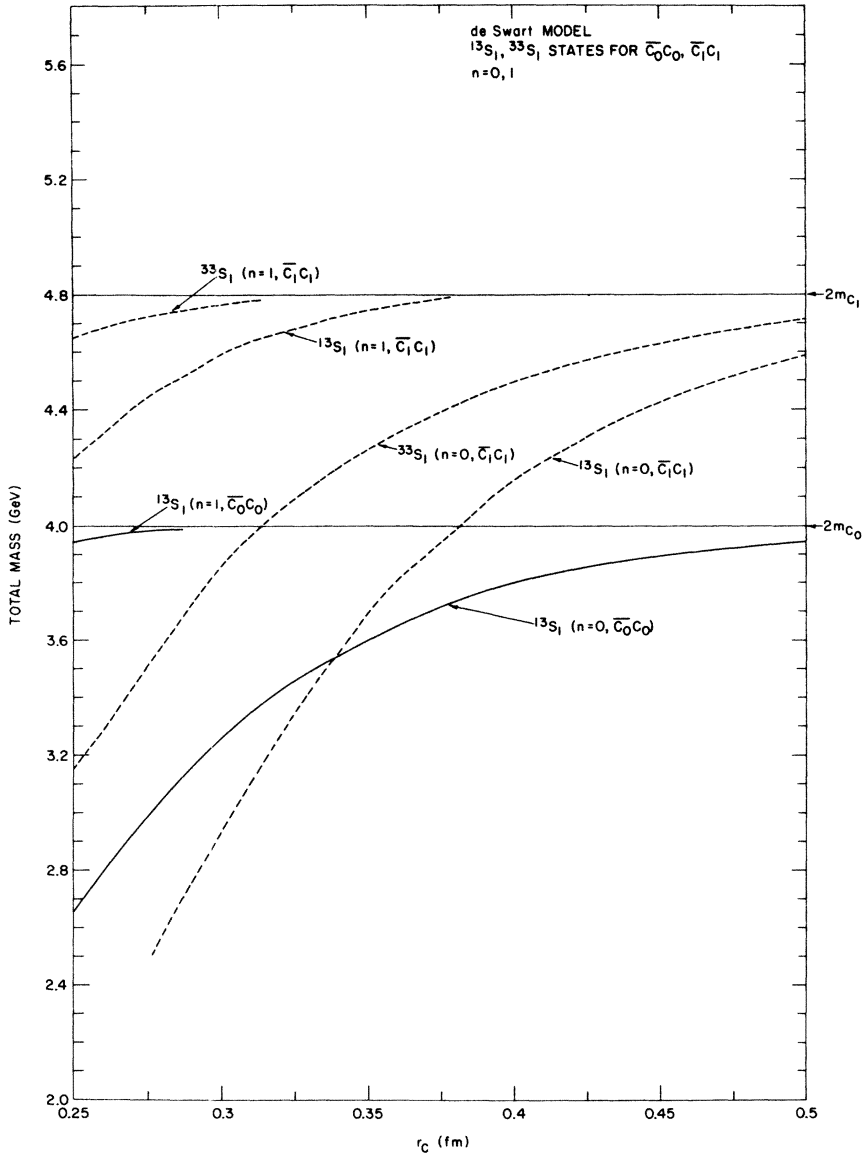

FIG. 3. Radial excitations ($n=1$) for the $^3S_1$ states of the $\bar{C}_0C_0$ and $\bar{C}_1C_1$ systems compared to nodeless states ($n=0$). We show the trajectories of such states as a function of the core radius r_c in the NRD model (Ref. 12). The thresholds are indicated by solid horizontal lines. Note that the mass of the C_0 has been taken to be 2 GeV in this figure; in the remainder of the figures, we use $m_{C_0}=2.26$ GeV.

very large rather close to threshold. Narrow $\bar{B}_cB_c$ resonant states are therefore much less likely than for the $\bar{N}N$ system, where they are in fact observed.[9]

The states in Fig. 2 correspond to nodeless wave functions ($n=0$). In Fig. 3, we display the energy of some $n=1$ radial $L=0$ excitations of the $\bar{C}_1C_1$ systems as a function of r_c in the NRD model. One sees that the spacing between $n=0$ and $n=1$ states depends fairly strongly on the absolute binding energy, and is of the order of 1 GeV. One can understand this in a simple way by recalling that the spacing between $L=0$ states with $n=0,1$ in a deep square well is given by[7]

$$\Delta\epsilon_n \approx \frac{3\pi^2}{m_B R^2}, \tag{3.3}$$

where R is the radius of the well. Taking $R\approx 0.7$ fm, we find $\Delta\epsilon_n$ of order 1 GeV for $\bar{C}_0C_0$ and $\bar{C}_1C_1$ systems, in qualitative agreement with Fig. 3. Thus we expect that only channels with rather deeply bound (≥ 1 GeV) $n=0$ states will also pos-

sess a bound $n=1$ state. Radial excitations of a quasimolecular nature thus seem rather unlikely for $L \geq 1$. Note also that the $n=0$, 1 splitting for $B_c B_c$ states is somewhat larger than that implied by the charmonium model (600 MeV); the size of the splitting clearly depends on the details of the radial shape of the potential, and will generally be smaller for more properly regularized potential models.

In our model, the energies of $L=0$ states are *extremely* sensitive to the details of the short-range cutoff. Because of the presence of the centrifugal barrier for configurations with $L \geq 1$, this sensitivity is reduced (although still considerable). Also, the barrier effect might be expected to lead to smaller widths for $L \geq 1$ states than for $L=0$ states (see Sec. IV). For these reasons, we place greater emphasis on predictions for $L \geq 1$ states in the remainder of this paper.

For $L=0$ states, there are no spin-orbit ($\vec{L}\cdot\vec{S}$) or diagonal tensor (S_{12}) forces. The binding is thus only due to the coherence of Wigner forces. For $L \geq 1$ states, $\vec{L}\cdot\vec{S}$ and S_{12} forces come into play, and produce large energy shifts for some $B_c B_c$ states. In Sec. II, we discussed the general features of the $\vec{L}\cdot\vec{S}$ and S_{12} splittings, in particular the role of the *coherence* of tensor forces. The influence of $\vec{L}\cdot\vec{S}$ and S_{12} forces on a typical $B_c B_c$ spectrum is illustrated by the "tree diagram" of Fig. 4 for the $L=1$ and 2 states of the $\bar{C}_0 C_0$ system. The left-hand column shows that these states are bound by central forces alone (see also Fig. 2). The middle column shows the result of adding $\vec{L}\cdot\vec{S}$ terms to the $\bar{C}_0 C_0$ potential; the effect is to depress the energy of $S=1$, $J=L-1, L$ states and raise the energy of $J=L+1$ states. This pattern of $\vec{L}\cdot\vec{S}$ shifts is due to the dominance of vector-meson $L\cdot S$ forces (mostly ω exchange) over scalar-meson $\vec{L}\cdot\vec{S}$ forces; this is true in all $B_c B_c$ systems within the class of models we have considered. In the right-hand column in Fig. 4, we have further added the effects of the diagonal part of the S_{12} force. Owing to its coherence properties for $\vec{T}_1\cdot\vec{T}_2 < 0$, the S_{12} force *always* shifts the $S=1$, $J=L-1$, $L+1$ states down and the $J=L$ state up in energy.

Since the $\vec{L}\cdot\vec{S}$ and S_{12} forces operate in opposite directions for $S=1$, $J=L$, $L+1$ states, the net effect is to position these states near the $S=0$, $J=L$ state, which is of course unshifted by $\vec{L}\cdot\vec{S}$ or S_{12} terms. Only the $I=0$, $S=1$, $J=L-1$ configuration is shifted downward by *both* spin-orbit and tensor forces. This is a general feature of all $I=0$ $B_c B_c$ systems.

For systems such as $\bar{C}_0 C_0$ and $\bar{T}T$, for which only $I=0$ mesons can be exchanged, $\vec{L}\cdot\vec{S}$ and S_{12} energy splittings are comparable in size. For

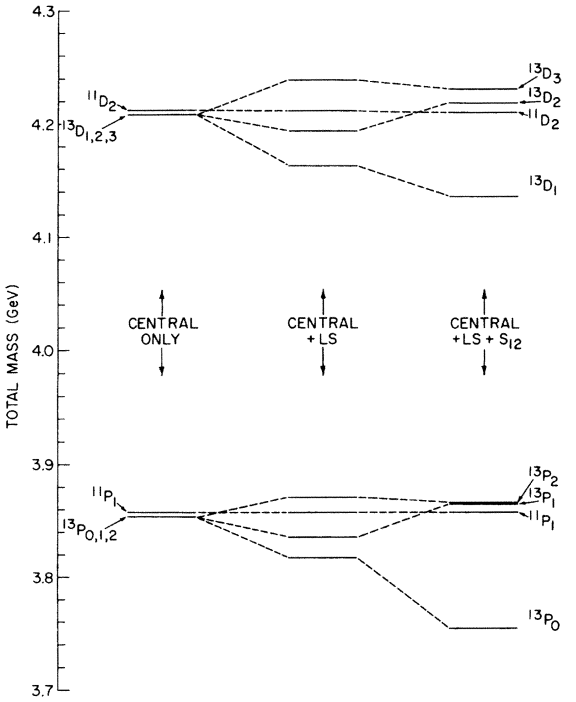

FIG. 4. Tree diagram for the $L=1,2$ states of the $\bar{C}_0 C_0$ system. We used the BP potential with $r_0 = 0.33$ fm. The first column shows the binding energies obtained with only the central part of the potential. The second column shows the result of adding the spin-orbit potential, while the third column displays the spectrum obtained including both spin-orbit and tensor forces.

systems such as $\bar{C}_1 C_1$, where $I=1$ mesons can also be exchanged, S_{12} splittings are generally somewhat larger than those from $\vec{L}\cdot\vec{S}$ forces, because of the coherence of tensor forces.

In Fig. 5, we illustrate the dependence of the $\bar{C}_0 C_0$ spectrum on the cutoff radius r_0 of the BP model. A value $r_0 = 0.6$ fm was used for the NN problem; the choice $r_0 = 0.456$ fm was taken for the $\bar{N}N$ system in Ref. 10, in connection with a suggestion that the $S(1930)$ meson[9] might correspond to a $^{11}D_2$, $^{31}D_2$ doublet of $\bar{N}N$ resonances. We use this same value $r_0 = 0.456$ fm for most of the calculations reported here. As seen in Fig. 5, this choice implies that the $L \geq 1$ states of the $\bar{C}_0 C_0$ system most likely lie above 4.2 GeV. Only by using a considerably smaller r_0 can one expect any $\bar{C}_0 C_0$ structure to appear in the vicinity of the ψ particle at 3.7 GeV. Note, however, that the coupling to the $\bar{C}_1 C_1$ system via pion exchange could considerably lower the energy of these states.

In Fig. 6, we give some indication of the cutoff and model dependence of the $\bar{C}_1 C_1$ spectrum. For sizable variations of the cutoff parameters r_0 and

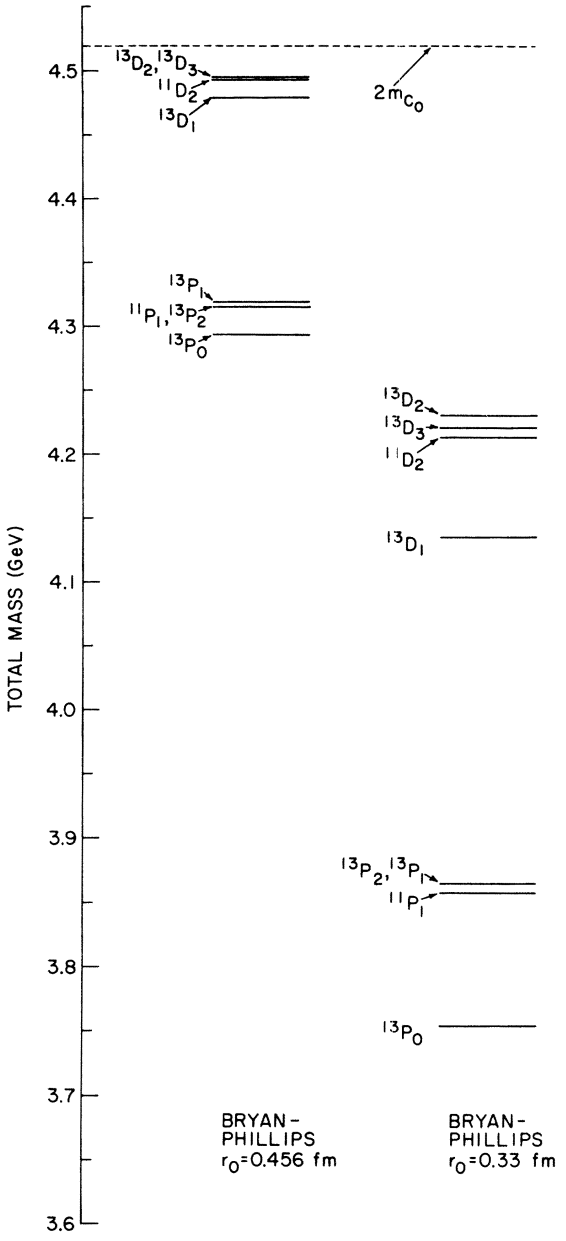

FIG. 5. Cutoff dependence of the $\bar{C}_0C_0$ spectrum ($L=1,2$ states). We used the BP potential with two choices for the cutoff radius r_0. Central, $\vec{L}\cdot\vec{S}$, and S_{12} forces are included. The $\bar{C}_0C_0$ threshold is indicated by a dashed line. The value $r_0=0.456$ fm was also used in Ref. 10 in connection with the $\bar{N}N$ problem.

r_c, all states with $L=1$ remain bound. Thus, although absolute binding energies vary by several hundred MeV for reasonable variations of r_0 and r_c, such nonrelativistic potential models support copious numbers of bound states.

Although the lowest threshold corresponds to $\bar{C}_0C_0$ at 4.52 GeV, some of the $\bar{C}_1C_1$ states with $I=0$ are much more strongly bound than $\bar{C}_0C_0$ states. This is due to strong, attractive $I=1$ exchange forces (π,ρ) for the $\bar{C}_1C_1$ system which are absent for $\bar{C}_0C_0$. Thus for a fixed value of r_0 or r_c, we expect $\bar{C}_1C_1$ states to constitute the lowest-lying part of the spectrum. However, these states may be strongly mixed with $\bar{C}_0C_0$ via π and ρ exchange. For $r_0=0.456$ fm, $\bar{C}_1C_1$ states occur in the (3–4)-GeV region. These could mix with $\bar{c}c$ states of the same quantum numbers. For larger r_0 or r_c (columns 2 and 4 of Fig. 6), these states could be physically distinct objects lying in the (4–4.5)-GeV region.

The lowest $\bar{C}_1C_1$ state with $L\neq 0$ is always $^{13}P_0$, as already predicted by general coherence arguments. For $\bar{C}_1C_1$, the coherence of tensor forces also holds for $I=1$ states, of which the lowest member must be the $J=L-1$ configuration, i.e., $^{33}P_0$. Since the vector-meson $L\cdot S$ forces (ρ,ω,φ) are also coherently attractive for this state, we expect on general grounds that the $^{33}P_0$ state will always be the second lowest $L=1$ state of the $\bar{C}_1C_1$ system, and of course the lowest $I=1$ state of any $\bar{B}_cB_c$ configuration. Figure 6 supports this claim. Note, however, that π and ρ exchange could strongly mix this configuration with $\bar{C}_1C_0$, which has a lower threshold.

The low-lying $\bar{C}_1C_1$ bound state in the $^{33}P_0$ channel is an interesting object; since it has $I=1$, it cannot be produced as a $\bar{c}c$ system. Its quantum numbers J^{PC} $(I^G)=0^{++}(1^-)$ correspond to those of the δ meson, i.e., an isovector scalar meson. Another interesting aspect of the $\bar{C}_1C_1$ spectra of Fig. 6 is the persistence of $I=2$ bound states near threshold. These states remain bound under very sizable variations of r_0 or r_c. Since they are generally weakly bound, their binding energies are not strongly dependent on cutoff. Such "exotic" $I=2$ configurations of $\bar{C}_1C_1$ may be ideal candidates for quasimolecular states; they are weakly bound, they have large rms radii, and many two-body decay channels are forbidden. The energies of $I=2$ mesons of $\bar{C}_1C_1$ type would lie between 4.5 and 4.8 GeV.

Some typical trajectories of binding energy vs r_0 for the BP model are shown in Fig. 7. The trajectories are rather flat for weakly bound states ($\leq$100-MeV binding) but are very steep for strong binding. Clearly any predictions for the binding energies of states below 4 GeV can change by several hundred MeV with rather modest changes in r_0.

A typical overall spectrum of $\bar{C}_0C_0$, $\bar{C}_1C_1$, and $\bar{S}S$ states below 4.5 GeV is shown in Fig. 8 for $r_0=0.456$ fm. As r_0 increases, the spectrum becomes more compressed; the lower states move up in energy most rapidly. Note that the only low-

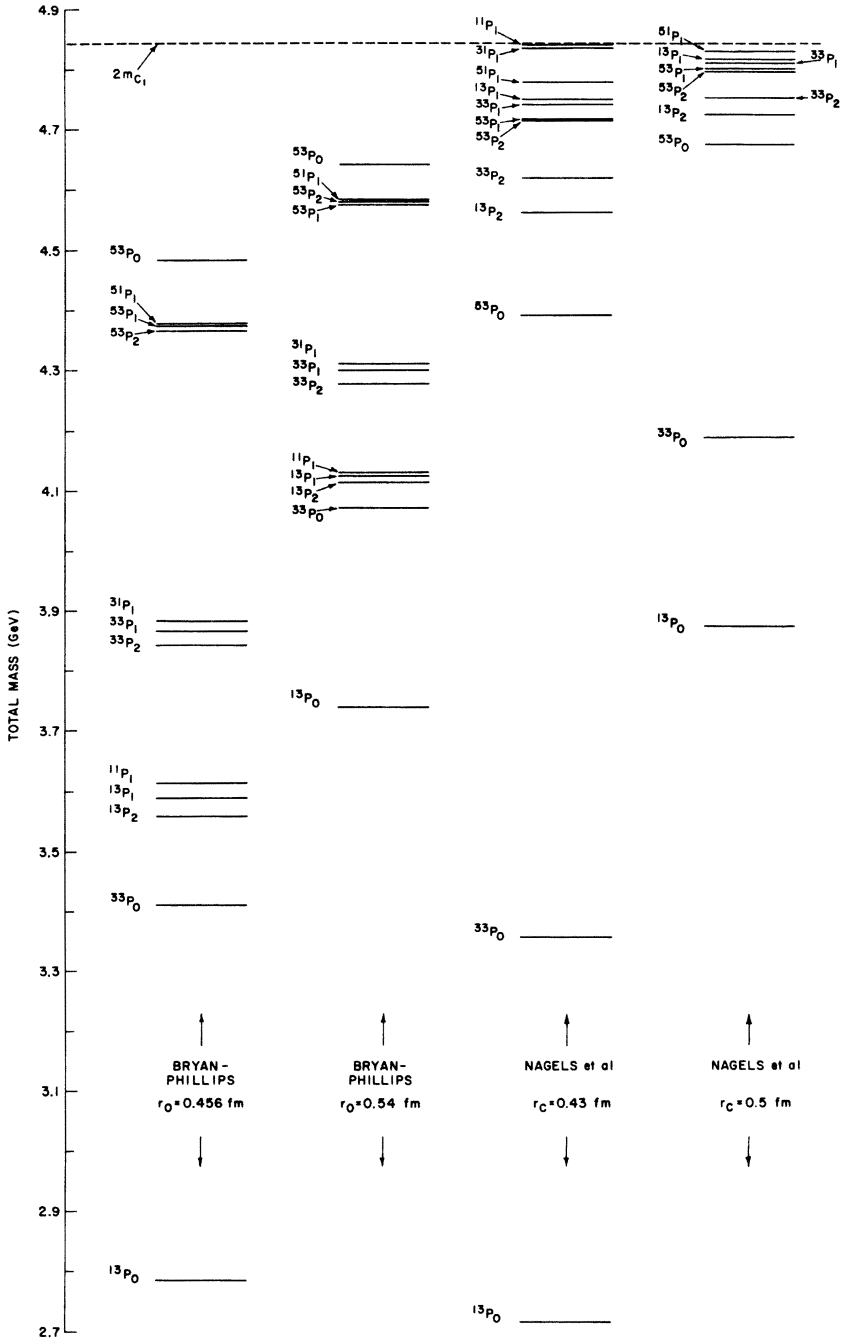

FIG. 6. The bound-state $L=1$ spectrum of the $\bar{C}_1C_1$ system for various potential models. Central, $\vec{L}\cdot\vec{S}$, and S_{12} forces have been included. The coupling constants used are those in Tables I and II for the BP and NRD models, respectively. The four columns correspond to different choices for the cutoff radii r_0 and r_c

lying $I=1$ state is the $^{33}P_0$ configuration of $\bar{C}_1C_1$. The $\bar{S}S$, $\bar{A}A$, and $\bar{X}X$ systems can generate high-lying $I=1$ states, but there is no coherence of either tensor- or vector-meson spin-orbit forces to bring these states down to low energy.

We now discuss the quasimolecular nature of $\bar{B}_cB_c$ states in more detail. In Fig. 9, we display the square of the radial wave function $u^2(r)$ for a typical $n=0$, $L=1$ state of a $\bar{B}_cB_c$ system. The wave functions are localized in r; the degree of localization is greater for more deeply bound states or for larger L. The bottom half of Fig. 9

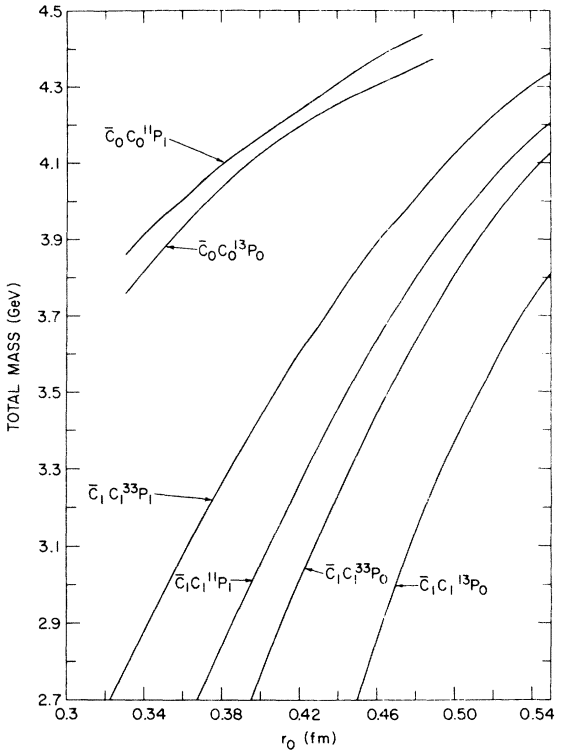

FIG. 7. Trajectories of typical $L=1$ bound states of the the $\bar{C}_0C_0$ and $\bar{C}_1C_1$ systems as a function of the cutoff radius r_0 for the BP potential $[V(r)=0$ for $r\leq r_0]$.

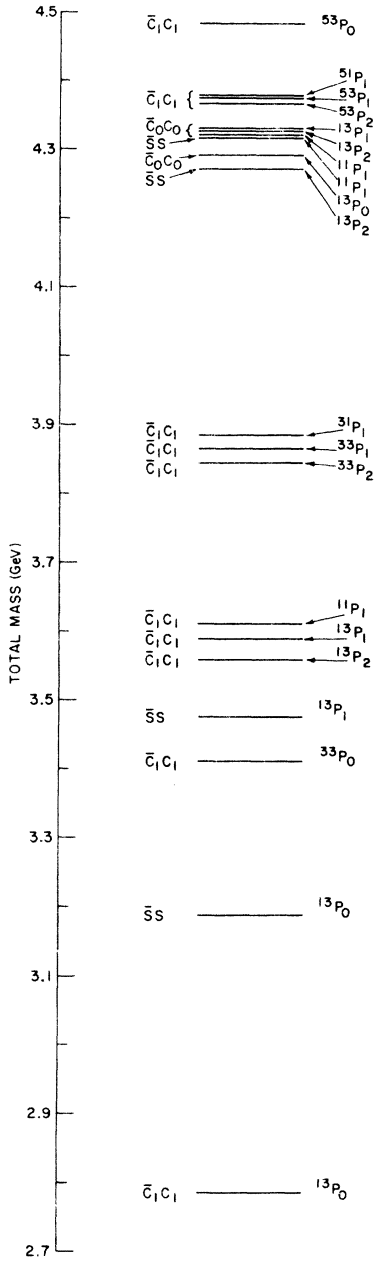

FIG. 8. Spectrum of all $L=1$ bound states below 4.5 GeV of the $\bar{C}_0C_0$, $\bar{C}_1C_1$, and $\bar{S}S$ system. Central, spin-orbit, and diagonal tensor forces are included. We used the BP potential with a common cutoff $r_0=0.456$ fm.

shows the rms radius $\langle r^2\rangle^{1/2}$ of the state as a function of binding energy ϵ_B. For weak binding, $\langle r^2\rangle^{1/2}$ varies as $\epsilon_B^{-1/2}$. For large binding ($\geq\frac{1}{2}$ GeV), further increases in binding produce only a very minor decrease of $\langle r^2\rangle^{1/2}$; this result may be an artifact of our particular form of cutoff. For $\epsilon_B<0.5$ GeV, however, we generally have $\langle r^2\rangle^{1/2}\geq 0.75$ fm. Since typical $\bar{c}c$ states have $\langle r^2\rangle^{1/2}\approx 0.3$–$0.5$ fm,[19] we have $\langle r^2\rangle_{\bar{B}_cB_c}^{1/2}>\langle r^2\rangle_{\bar{c}c}^{1/2}$. Thus our $\bar{B}_cB_c$ quasimolecules are localized at larger distances than charmonium states. If such $\bar{B}_cB_c$ states exist, they should thus be physically distinguishable from $\bar{c}c$ states. Note that for the weakly bound $I=2$ systems of $\bar{C}_1C_1$, we have $\langle r^2\rangle^{1/2}>1$ fm.

IV. EXPERIMENTAL CONSEQUENCES

The calculations described in the preceding sections strongly indicate the existence of a large number of quasimolecular $\bar{B}_cB_c$ bound states in the region below 4.8 GeV. Some of these states are predicted to have $I=1$, 2 in clear contrast with charmonium. ($I=1$ states are also predicted for quasimolecular $D\bar{D}$ systems,[6] but $I=2$ states are not.) Without more knowledge about the production and decay properties of charmed baryons themselves, it is not possible to make detailed predictions about similar properties for $\bar{B}_cB_c$ bound states. We are further handicapped in discussing the dynamics of quasimolecular states since nothing is known experimentally about the analogous $\bar{\Lambda}\Lambda$ and $\bar{\Sigma}\Sigma$ systems to guide us. Nevertheless, we will make some qualitative remarks which may be useful.

We have not emphasized the possibility of S

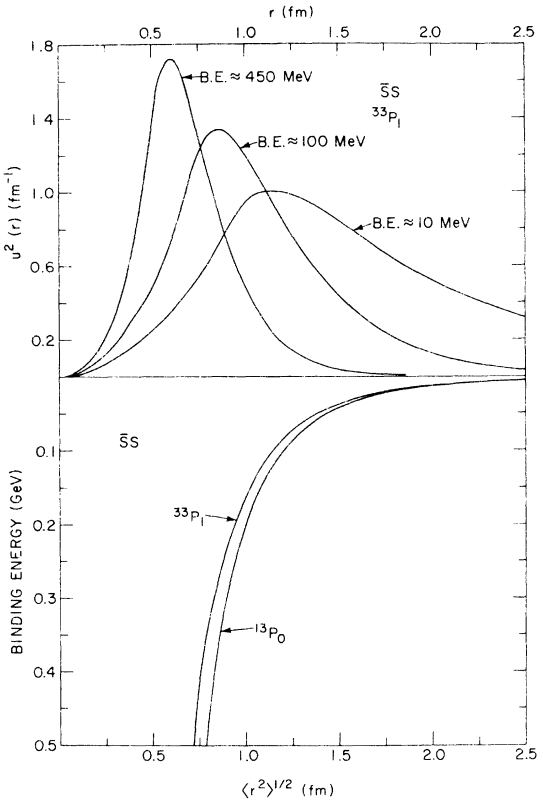

FIG. 9. Wave functions and rms radii for a typical $L=1$ bound state of $\bar{B}_c B_c$ type. We used the BP potential with central, $\vec{L}\cdot\vec{S}$, and S_{12} forces included. The cutoff radius r_0 was varied in order to change the binding energy. The top half of the figure shows the square of the radial wave function $u^2(r)$ as a function of r for three different binding energies. The bottom half exhibits the rms radius $\langle r^2\rangle^{1/2}$ as a function of binding energy for two typical $\bar{S}S$ states.

states mainly because the quasimolecular approximations used are most questionable for them. In particular, mixing with charmonium states and $D\bar{D}$ states is likely to play a significant role in the dynamics of S states. Nevertheless, we must expect some partly $\bar{B}_c B_c$ S states to exist and lie below the P states we have calculated. The most likely result of the production of the various $\bar{B}_c B_c$, P and D states is a cascade by π emission to the low-lying S states. The rate for these decays is mainly dependent on the energy separation, and since for the higher-lying states there are many possible paths for cascading, it is not possible to give a reliable estimate for the widths. Rough estimates using perturbation theory following, for example, Van Royen and Weisskopf[20] leads us to expect widths of at least 10 MeV and probably much more for these decays.[21] It is possible that for the lowest-lying P states other decays, of the sort to be discussed below, may be competitive with these but it is hard to be definitive about this.

A most interesting question, which we have not addressed, is the degree of mixing with charmonium states. This has many important experimental consequences and any data regarding these would be very useful in sorting out the dynamics. For one thing, it would control the rate at which the cascade terminates with J/ψ. An obvious decay to look for is

$$^{31}P_1 \to J/\psi + \pi\,.$$

A similar decay, probably somewhat less probable because P-state mixing with $\bar{c}c$ states should be less than S-state mixing, is

$$^{33}P_J \to \chi + \pi\,.$$

The mixing could also have a significant effect on the properties of the charmonium states. The $\bar{B}_c B_c$ states are expected to be more than twice as large as charmonium states.[19] Calculations for the charmonium states suggest that the J/ψ has a root-mean-square radius $R(J/\psi)\approx 0.28$ fm. This more or less is confirmed by the known $\psi'\to\chi\gamma$ and $\chi\to\psi\gamma$ electromagnetic decays.[22,23] Describing these states, for example, by harmonic-oscillator wave functions with a common size parameter yields $R(J/\psi)\lesssim 0.38 \pm 0.08$ fm. This combined with B_c carrying unit charge on the average, as opposed to $\frac{2}{3}$ for c, leads to $E1$ transitions approximately an order of magnitude larger than for charmonium. Thus a small admixture of $\bar{B}_c B_c$ into $c\bar{c}$ could profoundly affect the observed γ-ray widths and branching ratios for charmonium.

Let us now set aside the mixing question and ask: What else can happen to the lowest-lying $\bar{B}_c B_c$ S states? As always, we expect that getting rid of the charmed quarks will be the most inhibited stage in any decay. It is probably not as difficult as for J/ψ decay because there is the possibility of $c\bar{c}$ annihilating through one gluon here. This is partially compensated for by the larger size of the $\bar{B}_c B_c$ state and the recoupling required to put $c\bar{c}$ in the state with the quantum numbers of one gluon. The recoupling coefficients can be calculated and are not very much smaller than 1 so we estimate for this process very roughly

$$\Gamma = \Gamma_{J/\psi}\left(\frac{R_{J/\psi}}{R_{B_c\bar{B}_c}}\right)^3\left(\frac{1}{\alpha_S}\right)^4$$
$$\approx 80\,\Gamma_{J/\psi}\,.$$

Although this is considerably larger than the J/ψ width, it is still rather small and we expect that quark rearrangement into charmonium states or charmed mesons (if the $\bar{B}_c B_c$ state lies above 3.7 GeV) to be favored. Thus, one should look for

$$^{33}S_1 \to J/\psi + \pi$$

or

$$^{31}S_0 \to J/\psi + \pi + \pi \text{ or } \eta_c + \pi .$$

If we assume that the effective force between the $c\bar{c}$ is stronger than that holding the baryons together then, once the $\bar{B}_c B_c$ system has dropped into the S state, the propagation of $c\bar{c}$ should be governed by the gluon exchange potential and so they should form J/ψ or ψ' states at a rate comparable with the widths of the high-lying charmonium states, i.e., 30 MeV or so.[24]

Since we are starting with a state containing a baryon and an antibaryon, it is tempting to think that the decays will lead to a fairly large percentage of final states containing $\bar{p}p$, $\bar{\Lambda}\Lambda$, etc. However, if our last assumption above is correct, this will probably not be the case because the large momentum transfer involved in annihilating the $c\bar{c}$ quarks will tend to destroy any remnant of baryonlike wave functions of the remaining light quarks.

These states are likely to be difficult to produce. In principle, the triplet S and D states could be produced directly in e^+e^- annihilation. We estimate the rate for D states to be very small, with widths of order a few eV. The rate for S states is again very dependent on the mixing with $c\bar{c}$. The wave function at the origin is smaller than for pure $c\bar{c}$ states and this, along with the form factors of the B_c, should reduce the rate by an order of magnitude from charmonium states. Alternatively, they could be produced in e^+e^- by first producing a high-lying charmonium state which decays into a $\bar{B}_c B_c$ state. This is probably rare, but it would be interesting to look for.

On the grounds that a $\bar{B}_c B_c$ state is more likely to be found in a process where charmed baryons have already been seen, photoproduction or neutrino production seem likely processes to investigate. Finally, in spite of Regge estimates to the contrary,[25] we cannot avoid the feeling that a good way to look for $\bar{B}_c B_c$ states is to start with $\bar{p}p$ states.

ACKNOWLEDGMENTS

We would like to thank D. P. Sidhu and F. Paige for useful discussions.

APPENDIX

Here we outline the calculations of the Yukawa coupling constants as determined by SU(4) invariance. The calculation is straightforward, but we include this outline so the interested reader can see how we obtained the coupling constants used in the potentials.

For our purposes, we need the couplings only to the neutral, nonstrange, noncharmed mesons. Since all the exchanged mesons are supposed to lie in SU(4) 15-plets or singlets, we need consider only the case of pseudoscalars explicitly. The scalar and vector couplings can be obtained by substitution of the corresponding mesons. There are then four mesons to consider, the $I=1$ π^0 and three $I=0$ η's, an SU(4) singlet, an SU(3)-singlet member of the 15-plet, and a member of the SU(3) octet. So we will calculate the couplings to

$$\begin{aligned}
\pi^0 &= \frac{1}{\sqrt{2}}(u\bar{u} - d\bar{d}) , \\
\eta_1 &= \frac{1}{\sqrt{4}}(u\bar{u} + d\bar{d} + s\bar{s} + c\bar{c}) , \\
\eta_8 &= \frac{1}{\sqrt{6}}(u\bar{u} + d\bar{d} - 2s\bar{s}) , \\
\eta_{15} &= \frac{1}{\sqrt{12}}(u\bar{u} + d\bar{d} + s\bar{s} - 3c\bar{c}) .
\end{aligned} \tag{A1}$$

TABLE III. Baryon wave functions.

$$\begin{aligned}
p &= \frac{1}{\sqrt{6}} T^{ud;u} \\
n &= \frac{1}{\sqrt{6}} T^{ud;d} \\
\Sigma^+ &= \frac{1}{\sqrt{6}} T^{us;u} \\
\Sigma^0 &= \frac{1}{\sqrt{12}}(2T^{us;d} - T^{ud;s}) \\
\Sigma^- &= \frac{1}{\sqrt{6}} T^{ds;d} \\
\Lambda &= \frac{1}{\sqrt{4}} T^{ud;s} \\
C_1^{++} &= \frac{1}{\sqrt{6}} T^{uc;u} \\
C_1^{+} &= \frac{1}{\sqrt{12}}(2T^{uc;d} - T^{ud;c}) \\
C_1^{0} &= \frac{1}{\sqrt{6}} T^{dc;d} \\
C_0^{+} &= \frac{1}{\sqrt{4}} T^{ud;c} \\
A^+ &= \tfrac{1}{2} T^{us;c} \\
A^0 &= \tfrac{1}{2} T^{ds;c} \\
S^+ &= \frac{1}{\sqrt{12}}(2T^{uc;s} - T^{us;c}) \\
S^0 &= \frac{1}{\sqrt{12}}(2T^{dc;s} - T^{ds;c}) \\
X^{++} &= \frac{1}{\sqrt{6}} T^{uc;c} \\
X^{+} &= \frac{1}{\sqrt{6}} T^{dc;c} \\
X_S^{+} &= \frac{1}{\sqrt{6}} T^{sc;c} \\
T^0 &= \frac{1}{\sqrt{6}} T^{sc;s}
\end{aligned}$$

A calculation of these couplings has already been published by Campbell,[26] but we disagree with the signs of many of the couplings he lists. Our signs agree with those given by Gell-Mann[27] for the non-charmed baryons, while Campbell's disagree with some of those as well. Mixing of the η's will be considered later.

The baryons are supposed to lie in the $\underline{20}$ representations of SU(4). The baryons are given by tensors which are constructed from quark fields according to

$$T^{\alpha\gamma;\beta} = q_\alpha q_\beta q_\gamma + q_\beta q_\alpha q_\gamma - q_\gamma q_\beta q_\alpha - q_\beta q_\gamma q_\alpha . \tag{A2}$$

These are tabulated in Table III. The meson tensors are the standard ones:

$$M_\beta{}^\alpha = q_\alpha \bar{q}_\beta ; \tag{A3}$$

these are tabulated in Table IV.[28]

Because $\underline{15} \otimes \underline{20}$ contains the baryon $\underline{20}$ twice, there are two independent couplings, just as in SU(3). Thus there are no new unknowns; the couplings are determined by the πNN coupling and the D/F ratio. We will use invariant products of tensors in order to construct the possible couplings. The baryon tensors satisfy

$$T^{\alpha\gamma;\beta} = -T^{\gamma\alpha;\beta} \tag{A4}$$

and

$$T^{\alpha\gamma;\beta} + T^{\beta\alpha;\gamma} + T^{\gamma\beta;\alpha} = 0 . \tag{A5}$$

Equation (A5) plays the role of the traceless condition on the meson 15-plet tensor $M_\beta{}^\alpha$ and reduces the number of independent components from 24 to 20.

The two invariant couplings are written so as to reduce to the standard D and F form for the non-charm particles:

$$\begin{aligned}\mathcal{L}_{\rm int} = \frac{\sqrt{2}}{6} g \{ & \alpha [\tfrac{1}{2} (T^{\alpha\beta;\delta})^\dagger T^{\alpha\beta;\gamma} M_\gamma{}^\delta - (T^{\rho\beta;\gamma})^\dagger T^{\alpha\beta;\gamma} M_\alpha{}^\rho] \\ & + (1-\alpha)[\tfrac{1}{2} (T^{\alpha\beta;\delta})^\dagger T^{\alpha\beta;\gamma} M_\gamma{}^\delta \\ & + (T^{\rho\beta;\gamma})^\dagger T^{\alpha\beta;\gamma} M_\alpha{}^\rho]\} .\end{aligned} \tag{A6}$$

It is now just a matter of substituting into (A6) from Tables III and IV to get the couplings. These are presented in Table V. In addition to these couplings, there is also the 16th meson, the SU(4) scalar η_1, which couples with a universal strength g_1 to all baryons.

We will assume that the putative η_c is nearly pure $c\bar{c}$ and that the observed η and η' contain very small amounts of $c\bar{c}$. For our calculations we will, in fact, treat them as totally unmixed in charm. The η_c, since it is so heavy, will not be included in our potential, so we need only the η and η' couplings. Now

$$\frac{u\bar{u} + d\bar{d} + s\bar{s}}{\sqrt{3}} = \frac{\sqrt{3}\,\eta_1 + \eta_{15}}{2} , \tag{A7}$$

so

$$\begin{aligned}\eta &= -\sin\theta \left(\frac{\sqrt{3}\,\eta_1 + \eta_{15}}{2} \right) + \cos\theta\, \eta_8 , \\ \eta' &= \cos\theta \left(\frac{\sqrt{3}\,\eta_1 + \eta_{15}}{2} \right) + \sin\theta\, \eta_8 .\end{aligned} \tag{A8}$$

Here the mixing angle is the usual SU(3) mixing

TABLE IV. Meson wave functions.

$$\pi^0 = \frac{1}{\sqrt{2}} (M^u_u - M^d_d)$$

$$\eta_8 = \frac{1}{\sqrt{6}} (M^u_u + M^d_d - 2M^s_s)$$

$$\eta_{15} = \frac{1}{\sqrt{12}} (M^u_u + M^d_d + M^s_s - 3M^c_c)$$

$$\eta_1 = \frac{1}{\sqrt{4}} (M^u_u + M^d_d + M^s_s + M^c_c)$$

TABLE V. Yukawa couplings.

	π^0	η_8	η_{15}
$N\bar{N}$	g	$\frac{1}{\sqrt{3}}(3-4\alpha)g$	$\frac{1}{\sqrt{6}}(3-4\alpha)g$
$\Sigma\bar{\Sigma}$	$2(1-\alpha)g$	$\frac{2}{\sqrt{3}}\alpha g$	$\frac{1}{\sqrt{6}}(3-4\alpha)g$
$\Lambda\bar{\Lambda}$	0	$-\frac{2}{\sqrt{3}}\alpha g$	$\frac{1}{\sqrt{6}}(3-4\alpha)g$
$\Xi\bar{\Xi}$	$(1-2\alpha)g$	$-\frac{1}{\sqrt{3}}(3-2\alpha)g$	$\frac{1}{\sqrt{6}}(3-4\alpha)g$
$C_1\bar{C}_1$	$2(1-\alpha)g$	$\frac{2}{\sqrt{3}}(1-\alpha)g$	$-\frac{1}{\sqrt{6}}(1-4\alpha)g$
$C_0\bar{C}_0$	0	$\frac{2}{\sqrt{3}}(1-\frac{5}{3}\alpha)g$	$-\frac{1}{\sqrt{6}}(1+\frac{4}{3}\alpha)g$
$S\bar{S}$	$(1-\alpha)g$	$-\frac{1}{\sqrt{3}}(1-\alpha)g$	$-\frac{1}{\sqrt{6}}(1-4\alpha)g$
$A\bar{A}$	$(1-\frac{5}{3}\alpha)g$	$-\frac{1}{\sqrt{3}}(1-\frac{5}{3}\alpha)g$	$-\frac{1}{\sqrt{6}}(1+\frac{4}{3}\alpha)g$
$X\bar{X}$	$(1-2\alpha)g$	$\frac{1}{\sqrt{3}}(1-2\alpha)g$	$-\frac{1}{\sqrt{6}}(5-4\alpha)g$
$X_S\bar{X}_S$	0	$-\frac{2}{\sqrt{3}}(1-2\alpha)g$	$-\frac{1}{\sqrt{6}}(5-4\alpha)g$
$T\bar{T}$	0	$-\frac{4}{\sqrt{3}}(1-\alpha)g$	$-\frac{1}{\sqrt{6}}(1-4\alpha)g$
$\Sigma\bar{\Lambda}$	$-\frac{2}{\sqrt{3}}\alpha g$	0	0
$C_1\bar{C}_0$	$-\frac{2}{\sqrt{3}}\alpha g$	0	0
$S\bar{A}$	$-\frac{1}{\sqrt{3}}\alpha g$	$-\alpha g$	0

angle. Hence for any baryon B we have

$$g_{BB\eta} = -\frac{\sqrt{3}}{2}\sin\theta\, g_1 - \tfrac{1}{2}\sin\theta\, g_{BB\eta_{15}} + \cos\theta\, g_{BB\eta_8},$$

$$g_{BB\eta'} = \frac{\sqrt{3}}{2}\cos\theta\, g_1 + \tfrac{1}{2}\cos\theta\, g_{BB\eta_{15}} + \sin\theta\, g_{BB\eta_8},$$

where $g_{BB\eta_8}$ and $g_{BB\eta_{15}}$ may be read from Table V. Thus to calculate the exchange force for these meson multiplet we need four quantities, typically taken to be g, g_1, α, θ. These have been obtained in a number of ways and the values used in our calculations are given in the text.

---

*Work supported by U. S. Energy Research and Development Administration.

[1]J. J. Aubert *et al.*, Phys. Rev. Lett. 33, 1404 (1974); J.-E. Augustin *et al.*, *ibid.* 33, 1406 (1974).

[2]T. Appelquist and H. D. Politzer, Phys. Rev. Lett. 34, 43 (1975); J. Kogut and L. Susskind, Phys. Rev. D 12, 2821 (1975); A. De Rújula and S. Glashow, Phys. Rev. Lett. 34, 46 (1975); E. Eichten, K. Gottfried, T. Kinoshita, J. Kogut, K. D. Lane, and T.-M. Yan, *ibid.* 34, 369 (1975).

[3]E. G. Cazzoli *et al.*, Phys. Rev. Lett. 34, 1125 (1975); B. Knapp *et al.*, *ibid.* 37, 882 (1976).

[4]G. Goldhaber *et al.*, Phys. Rev. Lett. 37, 255 (1976); I. Peruzzi *et al.*, *ibid.* 37, 569 (1976).

[5]G. Feinberg and T. D. Lee, Phys. Rev. D 13, 3071 (1976).

[6]M. Bander, G. L. Shaw, P. Thomas, and S. Meshkov, Phys. Rev. Lett. 36, 695 (1976); C. Rosenzweig, *ibid.* 36, 697 (1976); S. Nussinov and D. Sidhu, BNL Report No. 22132 (unpublished); A. De Rújula, H. Georgi and S. Glashow, Phys. Rev. Lett. 38, 317 (1977).

[7]O. D. Dalkarov, V. B. Mandelzweig, and I. S. Shapiro, Nucl. Phys. B21, 88 (1970); L. N. Bogdanova, O. D. Dalkarov, and I. S. Shapiro, Ann. Phys. (N.Y.) 84, 261 (1974); C. B. Dover, in *Proceedings of the Fourth International Symposium on $\bar{N}N$ Interactions*, Syracuse, 1975, edited by T. E. Kalogeropoulos and K. C. Wali (Syracuse Univ., Syracuse, New York, 1975), Vol. II, Chap. VIII, pp. 37–91; a list of references to earlier work on the $\bar{N}N$ system can be found here.

[8]G. Schierholz and S. Wagner, Nucl. Phys. B32, 306 (1971); G. Schierholz, Nuovo Cimento 16A, 187 (1973).

[9]A. S. Carroll *et al.*, Phys. Rev. Lett. 32, 247 (1974); T. E. Kalogeropoulos and G. S. Tzanakos, *ibid.* 34, 1047 (1975); L. Gray, P. Hagerty, and T. E. Kalogeropoulos, *ibid.* 26, 1491 (1971); V. Chaloupka *et al.*, Phys. Lett. 61B, 487 (1976).

[10]C. B. Dover and S. H. Kahana, Phys. Lett. 62B, 293 (1976); see also Ref. 7.

[11]C. B. Dover and M. Goldhaber, Phys. Rev. D 15, 1997 (1977).

[12]M. M. Nagels, T. A. Rijken, and J. J. de Swart, Phys. Rev. D 12, 744 (1975); 15, 2547 (1977).

[13]R. A. Bryan and A. Gersten, Phys. Rev. D 6, 341 (1972); T. Ueda and A. E. S. Green, Phys. Rev. 174, 1304 (1968); Nucl. Phys. B10, 289 (1969); see also the review by K. Erkelenz, Phys. Rep. 13c, 191 (1974).

[14]R. A. Bryan and R. J. N. Phillips, Nucl. Phys. B5, 201 (1968).

[15]R. A. Bryan and B. L. Scott, Phys. Rev. 177, 1435 (1969).

[16]N. P. Samios, M. Goldberg, and B. T. Meadows, Rev. Mod. Phys. 46, 49 (1974).

[17]M. Nagels, T. A. Rijken, and J. J. de Swart, Phys. Rev. Lett. 31, 569 (1973).

[18]A. De Rújula, H. Georgi, and S. L. Glashow, Phys. Rev. D 12, 149 (1975). We have increased all their predicted masses by about 0.06 GeV in order for C_0 and C_1 to agree with the experiments cited in Ref. 3.

[19]E. Eichten *et al.* (unpublished result quoted by Nussinov and Sidhu in Ref. 6); cf. also Sec. IV.

[20]R. Van Royen and V. F. Weisskopf, Nuovo Cimento 50A, 617 (1967).

[21]For example, single-π emission in the transition $^3S_1 \to {}^1S_1 + \pi$ possesses a width $\approx$10 MeV when the energy separation between the states is $2m_\pi$.

[22]G. Feldman *et al.*, Phys. Rev. Lett. 35, 821 (1975); W. Tanenbaum *et al.*, *ibid.* 35, 1323 (1975).

[23]J. D. Jackson, Phys. Rev. Lett. 37, 1107 (1976).

[24]J. Siegrist *et al.*, Phys. Rev. Lett. 36, 700 (1976).

[25]V. Barger and R. J. N. Phillips, Phys. Rev. D 12, 2623 (1975); R. Field and C. Quigg, Report No. FNAL-75/15 THY (unpublished); D. P. Sidhu, T. L. Trueman, and L. L. Wang, Brookhaven Report No. PD-124 (unpublished).

[26]George Campbell, Jr., Phys. Rev. D 13, 462 (1976).

[27]M. Gell-Mann, Caltech Report No. CTSL-20, 1961 (unpublished).

[28]We use the nomenclature given by M. K. Gaillard, B. W. Lee, and J. L. Rosner, Rev. Mod. Phys. 47, 277 (1975).